



## Design A Battery Charger with Arduino Uno-Based for A Wind Energy Power Plant

A T Nugraha<sup>1\*</sup>, D Priyambodo<sup>1</sup>, and S T Sanera<sup>2</sup>

<sup>1</sup> Department of Marine Electrical Engineering, Shipbuilding Institute of Polytechnic Surabaya, Jl. Teknik Kimia, Surabaya, 60111, Indonesia.

<sup>2</sup> Department of Electrical and Electronic Engineering, Faculty of Engineering, University of Nottingham, Nottingham, East Midlands, NG7 2RD, United Kingdom.

\*E-mail: [anggaranugraha@ppns.ac.id](mailto:anggaranugraha@ppns.ac.id)

Received  
21 September 2021

Revised  
31 March 2022

Accepted for Publication  
10 April 2022

Published  
18 April 2022



This work is licensed  
under a [Creative  
Commons Attribution-  
ShareAlike 4.0  
International License](https://creativecommons.org/licenses/by-sa/4.0/)

### Abstract

In 2019, fossil energy produced more than 88% of Indonesia's electrical energy. For this reason, innovation in supplying electrical energy via renewable energy is required. One of them is wind energy with a potential of 60.6 GW, which has only been utilized at 0.15 GW or only 0.25% of the existing potential. One of the essential components in this power plant is the battery. The process of charging the battery that is not suitable can cause a decrease in battery performance. Therefore, a battery charger is built that uses a buck converter to lower the voltage while employing PI control to regulate the output voltage. From system testing, it is found that the output voltage of the charge controller is stable, where the most significant error value from the output voltage value is 0.972%. The average output current from the buck converter test using the PI approach is 16.84 mA, while the average input current is 15.73 mA. As a result, this charge controller can improve the battery charger's charging efficiency and hence lengthen the battery's lifetime.

**Keywords:** wind, turbine, battery, Arduino Uno.

### 1. Introduction

Electricity is an essential need and is a resource needed in daily activities. The longer the need for electricity will increase along with the increase and development of both the population, regional development, and the increasing amount of investment. In addition, the government is also committed to making the best efforts for equitable distribution of electricity for the realization of equitable energy. This support by Ministerial Regulation No. 38, 2016, concerning the “Acceleration of Electrification in Undeveloped Rural Areas, Remote Areas, Borders, and Small Inhabited Islands through the Implementation of Small-Scale Electricity Supply Businesses” [1]. The effort makes to achieve 100% electrification ratio by 2024 following the Decree of the Minister of Energy and Mineral Resources of the Republic of Indonesia Number 1567, 2018, concerning the “Business Plan for the Provision of Electricity for PT Perusahaan Listrik Negara (Persero) from 2018 to 2027” [2]. On the other side, electricity demand expects to grow more than seven times to 1,611 TWh in 2050. [3]. However, in 2019 more than 88% of electricity energy in Indonesia is still generated by fossil energy, with around 60% from coal, 22 % from natural gas, 6% from oil, and only 12% produced from renewable energy [4]. Because fossil energy is a non-renewable energy source, it will run out if consumed indefinitely. In addition, the use of fossil energy will also cause air pollution and increase the greenhouse effect, which is harmful to public health [5]–[7]. For this reason, innovations require to continuously fulfil electrical energy in Indonesia by utilizing the potential of renewable energy.

Based on previous research, there are solutions to utilize wind energy potential in Indonesia. Wind speed in Indonesia classifies as low wind speed [8]. The potential for low-speed wind energy can utilize by using vertical wind turbines. This study aims to determine the performance of vertical wind turbines with variations in the number of blades used. The previous research results found that the fewer blades used in the manufacture of vertical wind turbines, the greater the rotational speed, but will have drawbacks, namely low torque moments and vice versa. In the previous study, wherein the high loading test, the efficiency value of the turbine with two blades had the lowest efficiency [9].

In previous research by Nugraha and Priyambodo [10], research was carried out on the angle of the vertical wind turbine blade placement, which carry out with four angle variations, *i.e.* 22.5°, 45°, -22.5°, and -45°. Where the purpose of the study is to find out how the position of the most efficient wind turbine blades. The research conducted finds that wind turbines can produce the highest power coefficient with a pitch angle of 45° and  $C_p$  max 7.39% with a TSR of 0.422 [10].

Furthermore, one of the essential components in this power plant is the battery, which functions as a store of energy generated from a vertical wind turbine [11]. After use, the battery needs to recharge. The recharging process of the battery that is not suitable can cause a decrease in battery performance. In a previous study [12], it was conducted on charger controllers using a buck converter. This research aims to design a charge controller for small scale utilization. Wherefrom the research conducted, it was found that the output voltage value of the charger controller was a maximum of 13.5 V with a maximum current output of 3 A.

In this research, a buck converter is used in a battery charger to reduce the voltage utilized to charge the battery. The output of the buck converter will be read by the current and voltage sensors, which will display on the LCD. In reading the current amount, the INA219 sensor is used, while the voltage value reading uses a voltage divider circuit. Sensor data processing is carried out by Arduino Uno using PI (Proportional Integral) control. Then the microcontroller will send data in the form of PWM to the driver to adjust the output of the buck converter. The PI control system regulates the output voltage stability of 14.4 V during the battery charging process. The advantage of using the PI method in this system is that it stabilizes the output voltage even though the input changes as the effect of the wind speed changes frequently.

Furthermore, the charge controller on the market for turbines does not include an interface for the system's input and output voltage values. So, the user must manually monitor to find out the input and output voltages on the system, and the system may involve a more complex system. This system can increase the effectiveness charging of the battery charger and extend the battery's lifetime.

## 2. Method

### 2.1. Calculation of Generated Power Potential

The calculation data is used in the selection of the generator. From the data collection of wind speed characteristics, it is found that the average wind speed is 4.037 m/s. From the speed value, it can be calculated the electric power potential generated by Equation 1 [13],

$$\begin{aligned} \left(\frac{P_{\text{sys}}}{A}\right) &= C_p \times \eta_{tr} \times \eta_g \times \eta_b \times \frac{1}{2} \times \rho \times v^3 & (1) \\ \left(\frac{P_{\text{sys}}}{A}\right) &= 0.4 \times 0.9 \times 0.75 \times 0.85 \times \frac{1}{2} \times 1,2 \text{ kg/m}^3 \times 4.037^3 \text{ m/s} \\ \left(\frac{P_{\text{sys}}}{A}\right) &= 7.486 \text{ W/m}^2 \end{aligned}$$

where  $P_{\text{sys}}/A$  is the power produced per unit area of the blade in  $\text{W/m}^2$  [13], [14],  $C_p$  is power coefficient,  $\eta_{tr}$  is transmission efficiency [15],  $\eta_b$  is battery efficiency [16],  $\eta_g$  is generator efficiency [17],  $\rho$  is air density in  $\text{kg/m}^3$  [18], and  $v$  is wind speed in m/s. From the calculations, it is found that the maximum power that can be generated is  $7.486 \text{ W/m}^2$ .

### 2.2. Work Principle

This part aims to support the performance of the tool made. The components used in the tool making process are shown in Figure 1. The chart is divided into input, process, and output. There is a voltage sensor, INA219 current sensor, and power output from the turbine as an electrical power source in the input section. Then, the process section consists of the Arduino Uno microcontroller board as a PWM producer and the part that processes input data from the voltage sensor and current sensor. In addition, a buck converter is useful for maintaining the power output that enters the battery to be constant and according to the planning that has been done. Lastly, the output consists of a battery and an LCD to display current and voltage output. This research controls the output voltage using PI control and determines the PI control design's value using analytical methods. The flowchart of the PI setting system at the output voltage of the buck converter is shown in Figure 2.

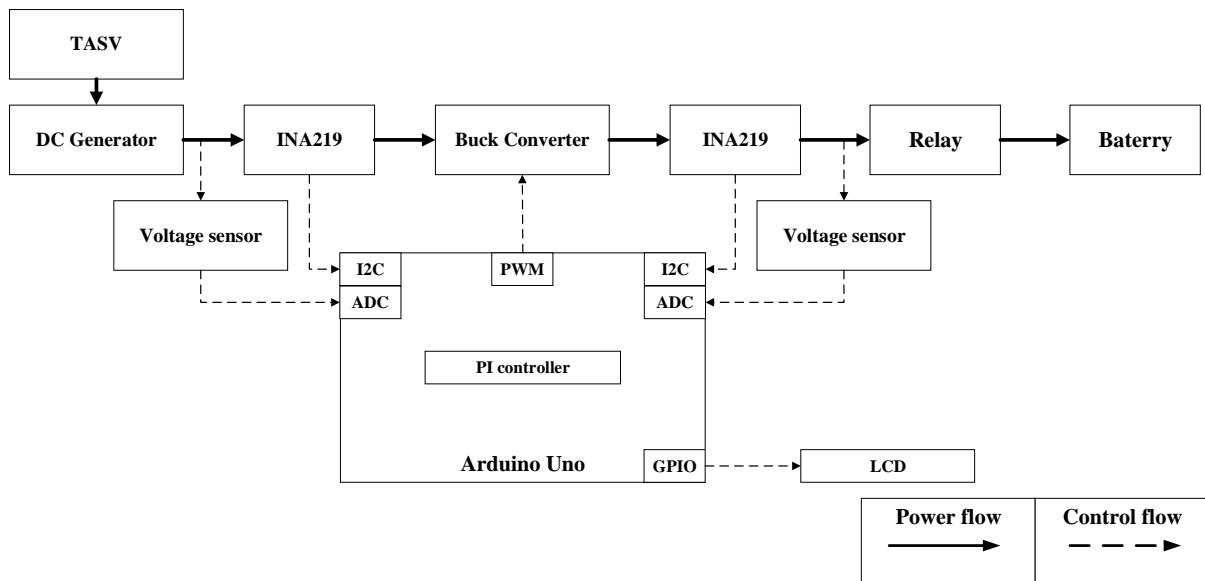


Figure 1. The components used in the tool making process.

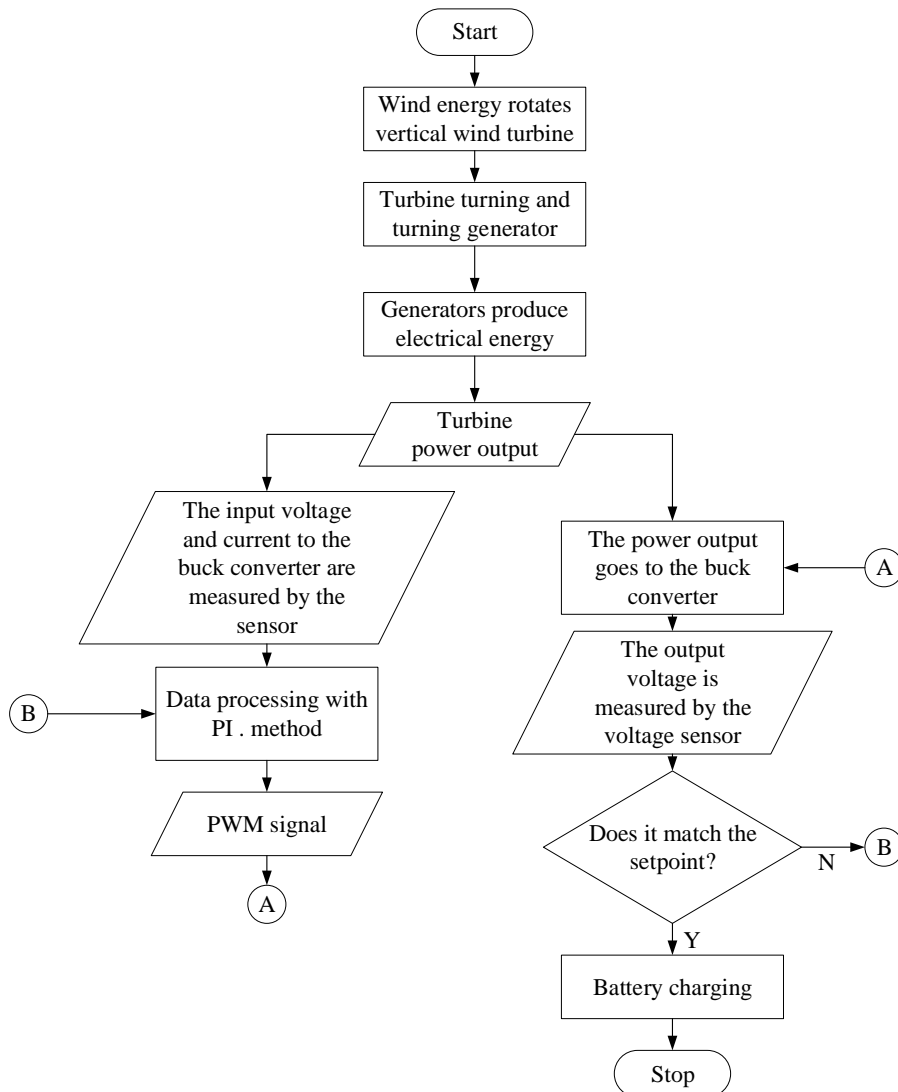
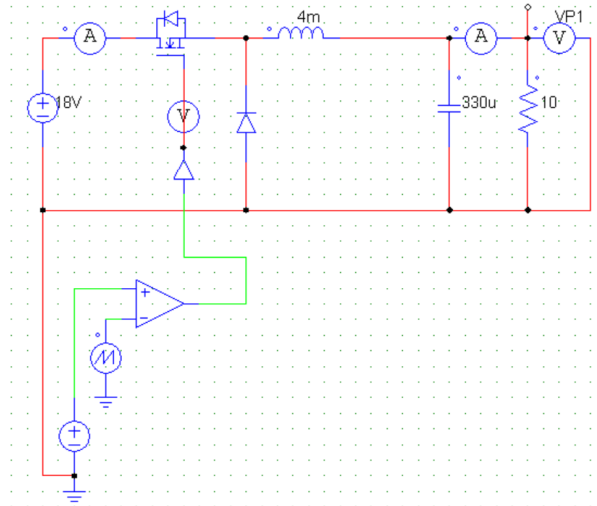


Figure 2. The flowchart of the PI setting system.



**Figure 3.** Buck converter circuit in PSIM application.

### 2.3. System Planning

The first step of system planning is to determine the value of and during the charging process. For the design of the PI control, it is necessary to know the results of the simulation waves under open-loop conditions. For this reason, a simulation of the buck converter circuit was carried out using the PSIM application. A series made on the PSIM application is shown in Figure 3.

From the circuit that has been made, run simulation is carried out and the output voltage waveform of the buck converter is known. Based on the simulation results of the open-loop buck converter as shown in the Figure 4, it is found that the response wave of the output voltage at steady state is 14.26 V with a steady state time of 66.89 ms. Based on the waves obtained in the above test, the following data were obtained as shown in Table 1. From the data output in Table 1, calculations are made to find the open-loop transfer function.

First, determine the gain over all ( $K$ ) value use Equation 2 [19].

$$K = \frac{Y_{ss}}{X_{ss}} = \frac{14.26 \text{ volts}}{14.40 \text{ volts}} = 0.99 \tag{2}$$

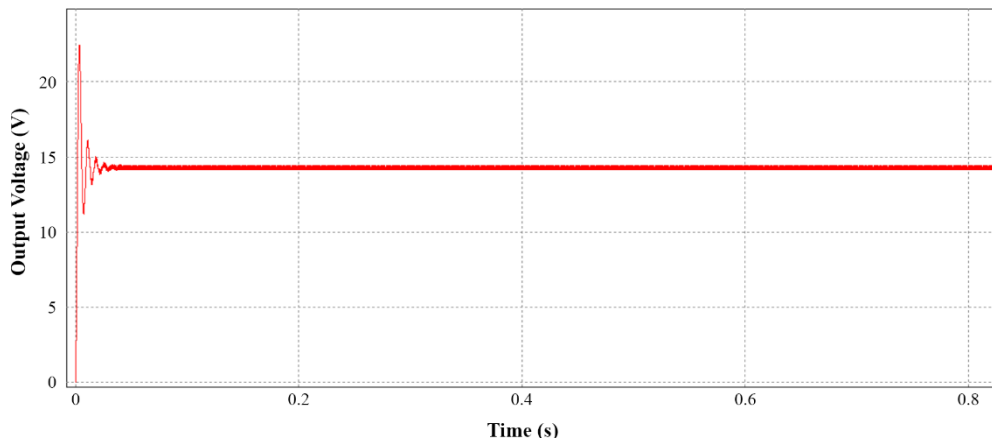


**Figure 4.** The output voltage waveform of the buck converter circuit.

**Table 1.** Data output of the buck converter circuit.

Output	Value
Steady state time ( $t_s$ )	0.06 s
Steady state voltage ( $Y_{ss}$ )	14.26 volts
Target voltage ( $X_{ss}$ )	14.40 volts

**Table 2.** Data output from the waves generated.

Output	Value
Setpoint ( $Y_{ss}$ )	14.40 volts
Peak wave ( $Y_p$ )	23.47 volts
Time to peak wave ( $t_{yp}$ )	0.0115 s

Then, determine of the time constant ( $\tau$ ) value by Equation 3 [20], [21] and Equation 4.

$$t_s = 5\tau \quad (3)$$

$$\tau = \frac{t_s}{5} = \frac{0.06 \text{ s}}{5} = 0.012 \text{ s} \quad (4)$$

The next step is to calculate the value of  $t_s^*$  by Equation 5 [15], [22] and Equation 6,

$$t_s^* = 5\tau \quad (5)$$

$$t_s^* = \frac{1}{n^*} \times t_s = \frac{1}{5} \times 0.06 \text{ s} = 0.012 \text{ s} \quad (6)$$

and we get the value of  $\tau^*$  (Equation 7) [16],

$$\tau^* = \frac{t_s^*}{n} = \frac{0,012 \text{ s}}{5} = 0,024 \text{ s} \quad (7)$$

The values of  $K_p$  (Equation 8) and  $K_i$  (Equation 9) in this system are [23],

$$K_p = \frac{\tau}{k \times \tau^*} = \frac{0,012 \text{ s}}{0.99 \times 0.024 \text{ s}} = 0.5050 \quad (8)$$

$$K_i = \frac{K_p}{\tau} = \frac{0.5050}{0.012} = 42.087 \quad (9)$$

From the calculations that have been carried out, it is found that the values of  $K_p$  and  $K_i$  are 0.5050 and 42.087, respectively.

Then, to perform tests on matlab, calculations must be carried out to obtain the transfer function of the open-loop buck converter circuit [24]. From the waves generated from the experiment using the PSIM application, we obtained data as shown in Table 2. The value of  $K$  is,

$$K = \frac{V_{\text{out}}}{\text{Duty Cycle}} = \frac{14.40}{0.80} = 18 \quad (10)$$

value of  $\zeta$  is [25],

$$\zeta = \frac{1}{\sqrt{1 + \left( \frac{\pi}{\ln\left(\frac{Y_p - Y_{ss}}{Y_{ss}}\right)}\right)^2}} = \frac{1}{\sqrt{1 + \left( \frac{3.14}{\ln\left(\frac{23.47 - 14.4}{14.4}\right)}\right)^2}} = 0.2523 \quad (11)$$

and value of  $\omega$  is [26],

$$\omega = \frac{\pi}{t_{Y_p} \times \sqrt{1 - \zeta^2}} = \frac{3.14}{0.0115 \times \sqrt{1 - 0.2523^2}} = 316.0577 \quad (12)$$

So, the open-loop transfer function of the buck converter circuit is

$$\text{OLTF buck converter} = \frac{1,798,064.644}{s^2 + 159.489 s + 99,892.48} \quad (13)$$

#### 2.4. Data Analysis

After the testing phase of the tool in the field and the tool runs smoothly, the data collection is carried out. After the experimental data are obtained in the field, the next stage of data analysis is carried out. This stage is carried out to determine the tool's performance and the tool's suitability with a predetermined system design.

##### 2.4.1. Simple Linear Regression Equation

The meaning of regression is estimation or forecasting. Regression analysis is useful for estimating the relationship between the value of one variable with another variable or can also be interpreted as an estimate of the statistical relationship between two or more variables. Simple linear regression analysis uses only two variables involved. The simple linear regression formula can be seen in Equation 14 [27], [28],

$$y = a + b(x) \quad (14)$$

where  $a$  is constant,  $b$  is regression coefficient,  $y$  is dependent variable, and  $x$  is independent variable. Where to find the values of  $a$  and  $b$  can use the Equation 15 and Equation 16 [25].

$$a = \frac{\Sigma Y - B \Sigma X}{n} \quad (15)$$

$$b = \frac{n \Sigma XY - \Sigma X \cdot \Sigma Y}{(n \Sigma XY)^2 - (\Sigma X)^2} \quad (16)$$

This method is used for the calibration phase of the INA219 sensor and the voltage sensor. The dependent variables of the voltage sensor and INA219 sensor are the voltage and current values measured on the multimeter. While the independent variable used is the result of reading the sensor value. From the two tests data, a linear regression formula was calculated using a graph in the excel application to find out the equations that appeared when the values of the two variables were entered.

##### 2.4.2. Error Percentage Value

This stage is carried out by comparing the data from measurements and calculations. By doing this, the error percentage will be found from the data that has been obtained. The percentage error value is the value obtained from the absolute value of the reduction in the actual value ( $N_a$ ) and the experimental value ( $N_e$ ) divided by the actual value ( $N_a$ ) and multiplied by 100%, as shown in Equation 17.

$$\text{Error (\%)} = \left| \frac{N_a - N_e}{N_a} \right| \times 100\% \quad (17)$$

##### 2.4.3. Error Average Value

The average error value is the value obtained from the division between the number of error values ( $\Sigma e$ ) and the amount of data ( $P$ ) [27], as shown in Equation 18.

$$\bar{x}e = \frac{\Sigma e}{P} \quad (18)$$



**Figure 5.** Wind speed data collection process.

### 3. Result and Discussion

#### 3.1. Wind Speed Test

Velocity data is collected at this stage, which is then used to carry out the design stage of the vertical axis wind turbine blades. This data collection was carried out by measuring the wind speed at Kenjeran Beach using an anemometer (Figure 5). This wind speed data collection was carried out on June 29, 2021, from 06.00 WIB to 18.00 WIB, recording data every hour. From the measurements that have been carried out, the following data were obtained, as shown in Table 3. Where from the data in Table 3, can be made a graph as shown in Figure 6.

**Table 3.** Wind speed test data.

No.	Time (WIB)	Wind Speed (m/s)
1.	06.00	2,70
2.	07.00	2,90
3.	08.00	3,32
4.	09.00	3,41
5.	10.00	3,52
6.	11.00	3,86
7.	12.00	4,20
8.	13.00	4,43
9.	14.00	4,76
10.	15.00	5,12
11.	16.00	5,53
12.	17.00	4,34
13.	18.00	4,40
Average		4,037

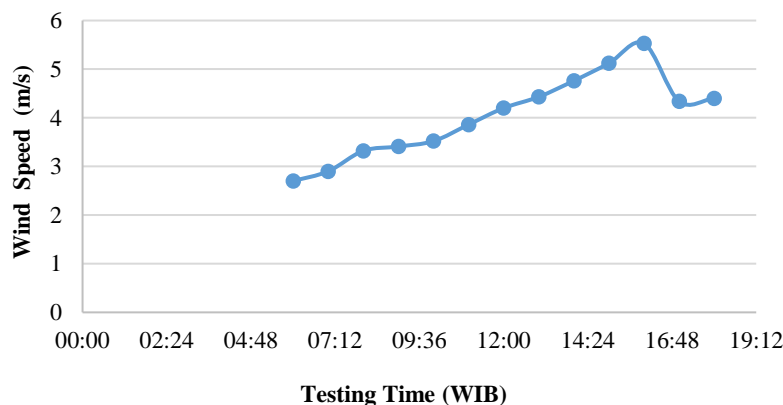


**Figure 6.** Wind speed measurement.

From the data in Table 3, it can be concluded that in the evening, the wind speed will be faster until 16.00 WIB, after which the wind speed will decrease and will be stable until the evening. Meanwhile, this test found that the lowest wind speed was at 06.00 WIB, which was 2.7 m/s. Meanwhile, the highest wind speed data is at 16.00 WIB, with a wind speed of 5.53 m/s. From testing the wind speed data, it was found that the average wind speed was 4.037 m/s.

### 3.2. Open-Loop Buck Converter Test

This test is conducted to determine the output of the buck converter when the system is not subjected to the PI method. Open-loop testing on the system integration of this converter is to use a resistive load at the output of the buck converter. This test is carried out using a duty cycle value of 80%. From the tests carried out, the data is shown in Table 4 and presented in a graph as shown in Figure 7.

From the tests carried out, it was found that the output voltage value of the buck converter in the test with an input voltage of 18.5 volts to 16.5 volts was below the setpoint (Figure 8). As for the input voltage of 19 V, the output voltage of the buck converter is above the setpoint. For this reason, it is necessary to use a method to improve the output voltage of the buck converter.

**Table 4.** Buck converter test data in open-loop.

$V_{in}$ (V)	$V_{out}$ (V)	$I_{in}$ (mA)	$I_{out}$ (mA)	$D$ (%)	Error $V_{out}$ (%)
19.0	15.05	15.3	17.1	79	4.514
18.5	13.57	15.2	17.0	73	5.764
18.0	14.32	15.4	17.4	80	0.556
17.5	13.95	15.4	17.1	80	3.125
17.0	13.57	15.5	17.1	80	5.764
16.5	13.20	15.3	17.0	80	8.333
Average					4.676

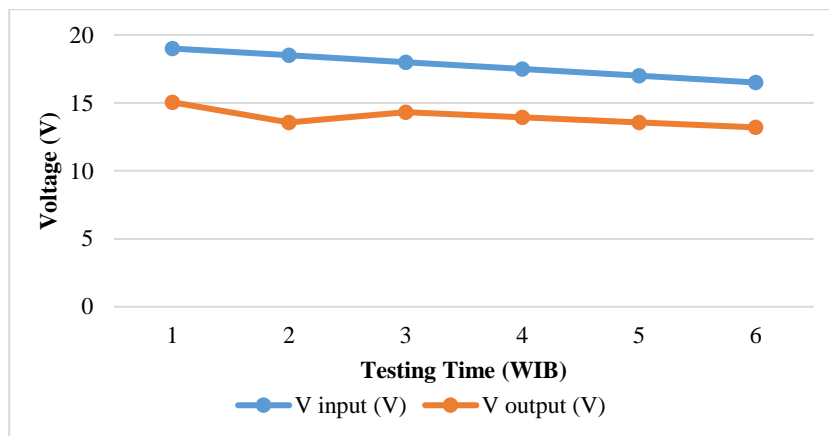


**Figure 7.** Open-loop buck converter charging data.



**Figure 8.** Open-loop buck converter test.

### 3.3. Buck Converter Test in Close-Loop without PI Method

This test is carried out by applying the duty cycle value where the duty cycle is obtained from reducing the set point value with the sensor reading value. The output voltage sensor in the circuit will be used as feedback which gives the reading of the voltage value in the system. From the tests carried out, the data is shown in Table 5 and presented in a graph as shown in Figure 9. The output voltage from the system test using closed control without any method. From the tests that have been carried out, it is found that the output value of the buck converter is unstable (Figure 10). This is because the duty cycle of the buck converter only depends on feedback and is not processed by a method.

### 3.4. Buck Converter Test with PI Method

The next buck converter test is to use the PI method. Where the  $K_p$  value used is 278. The results of the tests carried out can be seen in Table 6 and presented in a graph as shown in Figure 11. Based on the tests carried out, the output voltage of the buck converter is unstable (Figure 12). This is because the greater the value of  $K_p$  given, the system will work unstable or the system response will be isolated.

Table 5. Buck converter test data in close-loop.

$V_{in}$ (V)	$V_{out}$ (V)	$I_{in}$ (mA)	$I_{out}$ (mA)	$D$ (%)	Error $V_{out}$ (%)
19.0	15.31	13.9	27.4	80.6	6.319
18.5	14.91	14.1	28.1	80.6	3.542
18.0	14.72	14.3	30.7	81.8	2.222
17.5	14.31	14.2	30.6	81.8	0.625
17.0	13.92	14.4	29.9	81.9	3.333
16.5	13.65	14.3	30.3	82.7	5.208
Average					3.541

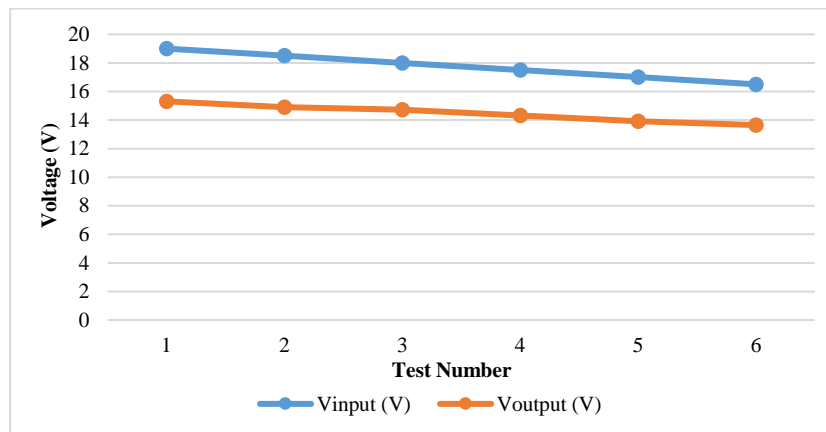


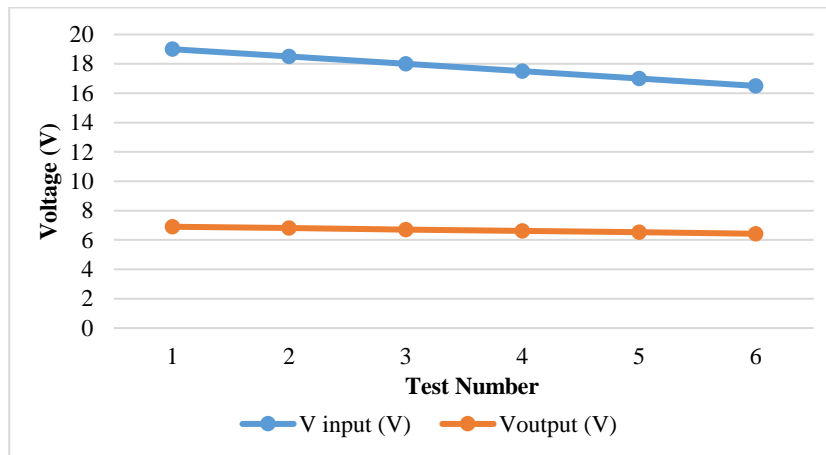
Figure 9. Close-loop buck converter test data.



Figure 10. Close-loop buck converter test.

**Table 6.** Buck converter test with PI method.

$V_{in}$ (V)	$V_{out}$ (V)	$I_{in}$ (mA)	$I_{out}$ (mA)	$D$ (%)	Error $V_{out}$ (%)
19.0	6.905	6.9	11.1	36.3	52.049
18.5	6.813	6.8	11.7	36.8	52.688
18.0	6.718	6.9	11.2	37.3	53.347
17.5	6.622	7.1	11.3	37.8	54.014
17.0	6.524	7.0	11.2	38.4	54.694
16.5	6.425	6.9	11.4	38.9	55.382
Average					53.690



**Figure 11.** Close-loop buck converter test data with PI method.



**Figure 12.** Buck converter test with PI method.

Based on [Table 6](#), the percentage error value of the system's output voltage is quite significant. This is because the small  $K_p$  value makes the buck converter's output unable to reach the set point.

### 3.5. Close-Loop Testing of Charger Controller with PI

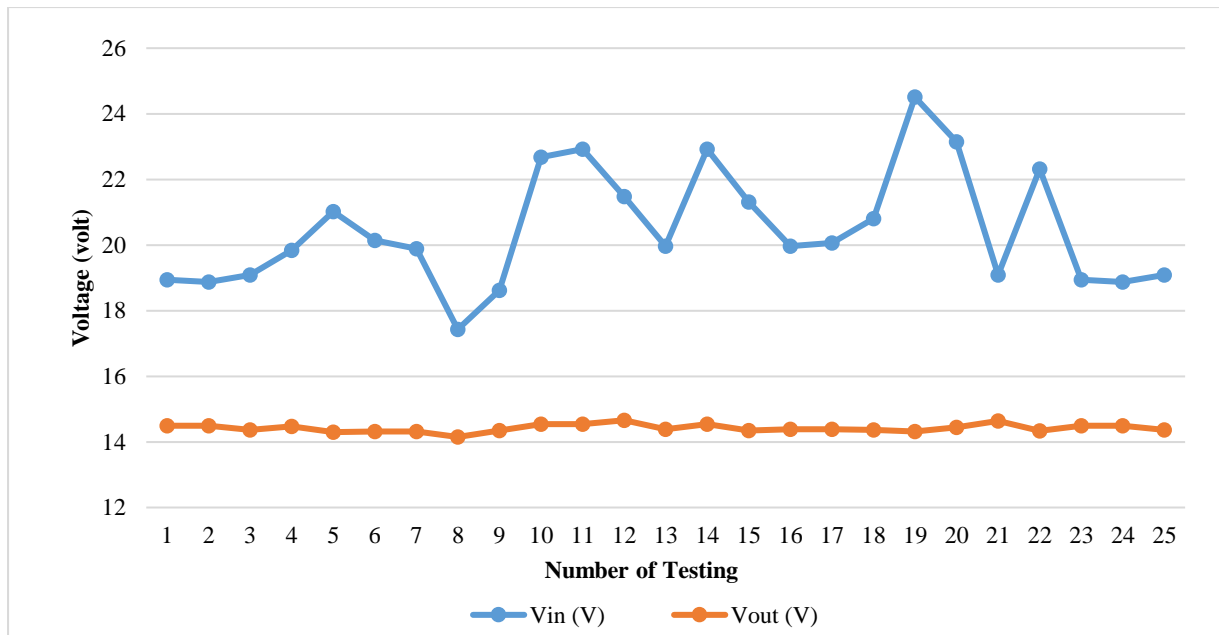
The PI control test aims to determine whether the system can maintain a constant voltage according to the design and compare the system when it is without control and when it is given control. The test is carried out using the input from the DC power supply, which is then inserted into the input of the buck converter. The load used during the simulation is a resistive load of 1 k $\Omega$ . This test is carried out using a random input voltage.

Meanwhile, when the test uses the value of  $K_p = 0.5050$  ([Equation 8](#)) and  $K_i = 42.087$  ([Equation 9](#)), where the determination to get the value uses the analytical method. Below is the buck converter simulation test data with open-loop and close-loop. From the experimental data on the PI control ([Table 7](#)), by varying the input voltage to find out how the response of the PI control, it proves that the use of PI control on the system is able to maintain the output voltage. The input and output voltage data on the buck converter test are presented in [Figure 13](#).

**Table 7.** Close-loop buck converter test data.

$V_{in}$ (V)	$V_{out}$ (V)	$I_{in}$ (mA)	$I_{out}$ (mA)	$D$ (%)	Efficiency (%)	Error (%)
18.94	14.49	1.8	2.1	77	89	0.625
18.87	14.49	2.1	2.3	77	84	0.625
19.09	14.37	2.2	2.3	75	79	0.208
19.84	14.47	1.9	2.3	73	88	0.486
21.02	14.30	2.1	2.4	68	78	0.694
20.14	14.32	2.0	2.1	71	75	0.556
19.89	14.32	2.1	2.6	72	89	0.556
17.43	14.15	1.9	2.3	81	98	1.736
18.62	14.35	2.0	2.5	77	96	0.347
22.68	14.54	1.6	2.0	64	80	0.972
22.92	14.54	2.0	2.7	63	86	0.972
21.48	14.66	1.8	2.4	68	91	1.806
19.97	14.39	2.2	2.6	72	85	0.069
22.92	14.54	2.0	2.9	63	92	0.972
21.31	14.35	2.0	2.8	67	94	0.347
19.97	14.39	2.0	2.3	72	83	0.069
20.06	14.39	1.9	2.6	72	98	0.069
20.81	14.37	1.8	2.1	69	81	0.208
24.51	14.32	2.0	2.4	58	70	0.556
23.15	14.44	1.8	2.2	62	76	0.278
19.09	14.64	1.9	2.5	77	101	1.667
22.32	14.34	2.1	2.4	64	73	0.417
18.94	14.49	1.8	2.1	77	89	0.625
18.87	14.49	2.1	2.3	77	84	0.625
19.09	14.37	2.2	2.3	75	79	0.208
Average				70	86	0.647

Based on Figure 13 and Figure 14, it is found that the average output voltage value is 14.48 V which is close to the value of the charging voltage on the planned battery, which is 14.40 V. From the tests that have been carried out, it is found that the buck converter can maintain the output voltage value in accordance with the constant voltage condition with an average error percentage of 0.647 % (Table 7).

**Figure 13.** Buck converter test.



**Figure 14.** Buck converter testing using the PI method.

### 3.6. Buck Converter Testing with Battery Load

System testing with a battery load (Figure 15) is carried out to know how long it takes to fully charge the battery and test the cut off module installed at the output of the charger controller, which is used to disconnect the circuit when the battery is full. In this charging simulation, a 7.2 Ah VRLA LC-R127R2CH battery is used. When testing the battery charging process, what must be considered is the initial SOC of the battery. In this test, the initial SOC is used at the time of charging, which is 12.3 V. For this reason, relay settings are made to charge when the battery voltage is 12 volts.

From the test data in Table 8, it is found that the system is capable of charging the battery. In this test, it can be seen that the system has been able to carry out the charging process on a battery. When the system is charging, the measured voltage will follow the cut-off relay's measured voltage (Figure 16). From this test, it is known that charging the battery from 50% to 100% SOC condition takes 23 minutes.

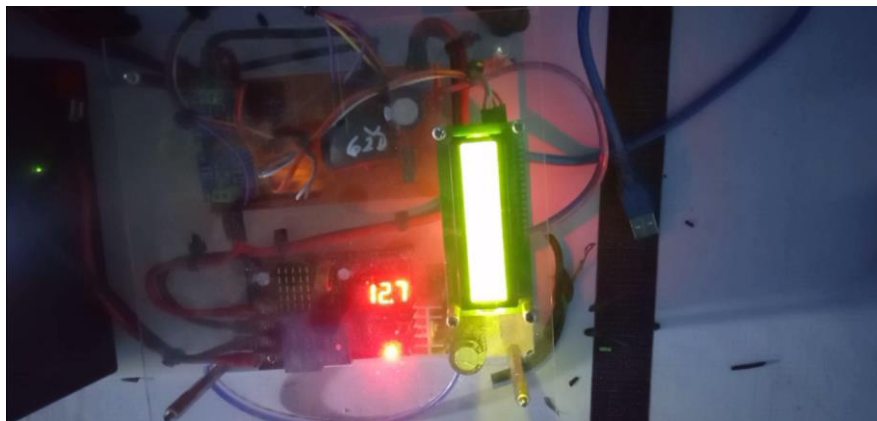


**Figure 15.** Buck converter test with battery load.

**Table 8.** Buck converter test data with battery load.

Time (minutes)	$V_{in}$ (V)	$I_{in}$ (A)	$V_{out}$ (V)	$I_{out}$ (A)	Relay Condition
0	18,33	0,949	12,3	1,146	On
3	18,46	0,89	12,4	1,139	On
7	18,69	0,824	12,5	1,074	On
12	18,53	0,739	12,6	0,957	On
18	18,43	0,635	12,7	0,814	On
23	18,32	0,618	12,8	0,780	Off

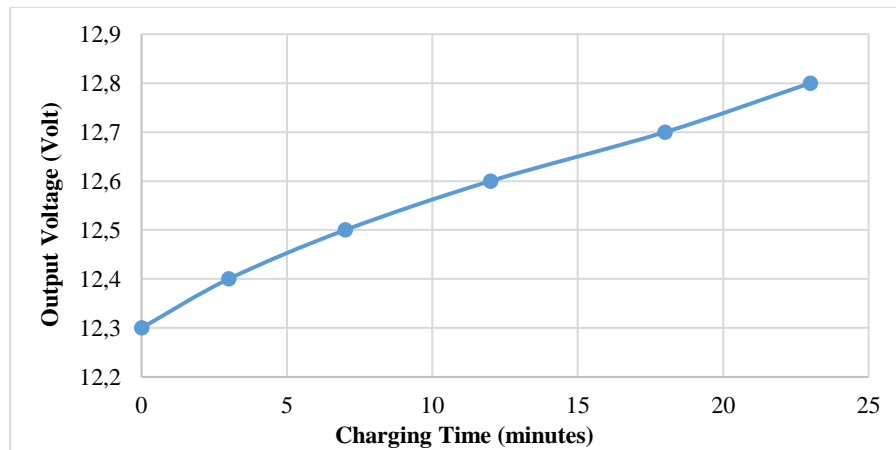


Figure 16. Battery charging test.

### 3.7. Integration Test with Wind Turbine

This test was carried out at Kenjeran Beach Surabaya, where this test was carried out by applying power input to the charger controller using a vertical wind turbine (Figure 17). On the other hand, observations were also made regarding the wind speed at Kenjeran Beach when this integration test was carried out. In this system, the input value of the buck converter from the vertical wind turbine will be measured and the value of the power output coming out of the buck converter will also be observed. The value of the input and output of the charger controller will be observed through the value displayed by the LCD. The test data that has been carried out can be seen in Table 9. From the tests carried out, it was found that charging the battery with an initial voltage of 12.3–12.8 V takes 31 minutes and the relay will turn off when the battery is full (Figure 18).



Figure 17. Charge controller integration test.

Table 9. Data integration test with wind turbine.

Time (minutes)	Wind Speed (m/s)	$V_{in}$ (V)	$I_{in}$ (A)	$V_{out}$ (V)	$I_{out}$ (A)	Relay Condition
0	4.2	17.63	1.23	12.3	1.25	On
4	4.3	17.81	1.32	12.4	1.36	On
8	4.1	17.51	1.27	12.5	1.35	On
12	4.2	17.71	1.38	12.6	1.41	On
16	3.9	17.49	0.95	12.7	1.14	On
20	3.9	17.52	0.79	12.7	0.84	On
24	3.6	16.43	0.72	12.7	0.81	On
28	3.7	16.71	0.64	12.8	0.72	On
31	3.7	16.38	0.05	12.8	0.02	Off

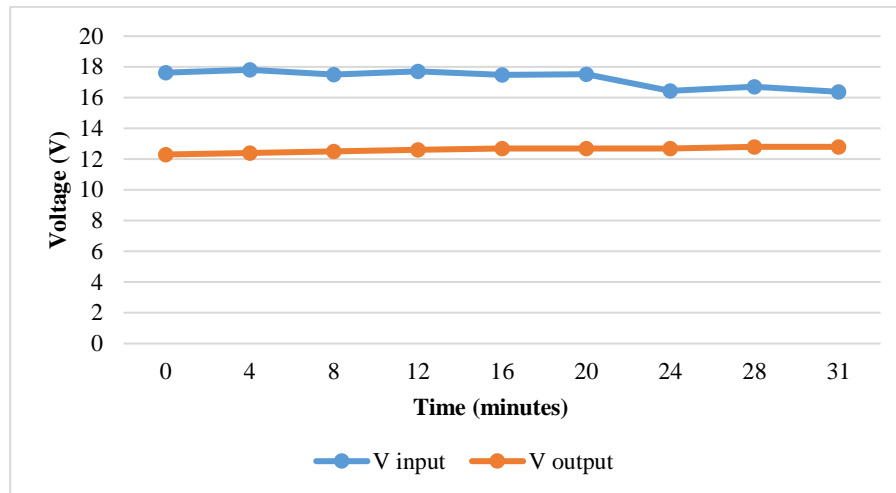


Figure 18. Charge controller integration test.

### 3.8. Discussion

The efficiency value of the buck converter obtained from this study is 85.115–95.154%. In addition, the output voltage of the charge controller becomes stable when the system is subjected to the PI method with an error percentage of 0.972%. The output current from the charge controller has a value greater than the input current, with an average output current of 16.84 mA, while the average input current is 15.73 mA. From the research done, it can be seen that the use of PI control can make the output voltage and buck converter stable. This tool has an input voltage limit of 25 V. When the voltage exceeds 25 V, the voltage sensor circuit will burn out. In addition, when the input voltage is greater than 25 V, the input voltage to the Arduino digital pin exceeds 5 V, which creates an overvoltage. The method used can make the voltage out of the buck converter more stable.

## 4. Conclusion

Based on data collection characteristics of wind speed, data obtained wind speed of 3.66 m/s and air density of 1.2 kg/m<sup>3</sup>. The power generated by the hybrid power plant is 95.47–101.62 Watt. From the research that has been done, it is found that the output voltage value of the battery charger made has an average error percentage of 1.373% and the power output efficiency of the battery charger is 83–95%. There is a need for research on calculating the type of ferrite material in the inductor and the magnitude of the switching frequency used in this charge controller to produce a more efficient output.

## References

- [1] Dutta, N. Barua, and A. Saha, “Design of an arduino based maximum power point tracking (MPPT) solar charge controller,” Dr. dissertation, Depart. Electr. Electron. Eng., Dhaka, BRAC University, 2016.
- [2] T. L. Floyd, *Electronic Devices (Electron Flow Version)*. New Jersey, U.S.A: Prentice Hall, 2012.
- [3] A. R. Gautam, D. M. Deshpande, A. Suresh, and A. Mittal, “A double input DC to DC buck-boost converter for low voltage photovoltaic/wind systems,” *Int. J. ChemTech Res.*, vol. 5, no. 2, pp. 1016–1023, 2013.
- [4] N. H. Baharudin, T. M. N. T. Mansur, F. A. Hamid, and M. I. Misrun, “Topologies of DC-DC converter in solar PV applications,” *Indones. J. Electr. Eng. Comput. Sci.*, vol. 8, no. 2, pp. 368–374, 2017, doi: [10.11591/ijeecs.v8.i2.pp368-374](https://doi.org/10.11591/ijeecs.v8.i2.pp368-374).
- [5] R. R. Gopi and S. Sreejith, “Converter topologies in photovoltaic applications—A review,” *Renew. Sust. Energ. Rev.*, vol. 94, pp. 1–14, 2018, doi: [10.1016/j.rser.2018.05.047](https://doi.org/10.1016/j.rser.2018.05.047).
- [6] M. Zagirnyak, V. Melnykov, and A. Kalinov, “The review of methods and systems of fault-tolerant control of variable-frequency electric drives,” *Przegląd Elektrotechniczny*, vol. 95, no. 1, pp. 141–144, 2019, doi: [10.15199/48.2019.01.36](https://doi.org/10.15199/48.2019.01.36).

- [7] V. Chenchevoi *et al.*, “Development of mathematical models of energy conversion processes in an induction motor supplied from an autonomous induction generator with parametric non-symmetry,” *EasternEuropean J. Enterp. Technol.*, vol. 4, no. 8, pp. 67–82, 2021, doi: [10.15587/1729-4061.2021.239146](https://doi.org/10.15587/1729-4061.2021.239146).
- [8] M. K. Kazimierczuk, *Pulse-Width Modulated DC–DC Power Converter*. Ohio, U.S.A: John Wiley & Sons, 2015.
- [9] A. T. Nugraha and D. Priyambodo, “Design of pond water turbidity monitoring system in arduino-based catfish cultivation to support sustainable development goals 2030 no. 9 industry, innovation, and infrastructure,” *J. Electron., Electromed. Eng., Med. Inform.*, vol. 2, no. 3, pp. 119–124, 2020, doi: [10.35882/jeeemi.v2i3.6](https://doi.org/10.35882/jeeemi.v2i3.6).
- [10] A. T. Nugraha and D. Priyambodo, “Design of a monitoring system for hydrogatics based on arduino uno R3 to realize sustainable development goals number 2 zero hunger,” *J. Electron., Electromed. Eng., Med. Inform.*, vol. 3, no. 1, pp. 50–56, 2021, doi: [10.35882/jeeemi.v3i1.8](https://doi.org/10.35882/jeeemi.v3i1.8).
- [11] M. A. Kabir and I. Husain, “Design of mutually coupled switched reluctance motors (MCSRMs) for extended speed applications using 3-phase standard inverters,” *IEEE Trans. Energy Convers.*, vol. 31, no. 2, pp. 436–445, 2015, doi: [10.1109/TEC.2015.2499086](https://doi.org/10.1109/TEC.2015.2499086).
- [12] E. Bostanci, M. Moallem, A. Parsapour, and B. Fahimi, “Opportunities and challenges of switched reluctance motor drives for electric propulsion: A comparative study,” *IEEE Trans. Transp. Electrification*, vol. 3, no. 1, pp. 58–75, 2017, doi: [10.1109/TTE.2017.2649883](https://doi.org/10.1109/TTE.2017.2649883).
- [13] M. Cheng and Y. Zhu, “The state of the art of wind energy conversion systems and technologies: A review,” *Energy Convers. Manag.*, vol. 88, pp. 332–347, 2014, doi: [10.1016/j.enconman.2014.08.037](https://doi.org/10.1016/j.enconman.2014.08.037).
- [14] A. T. Nugraha and D. Priyambodo, “Prototype hybrid power plant of solar panel and vertical wind turbine as a provider of alternative electrical energy at Kenjeran beach Surabaya,” *J. Electron., Electromed. Eng., Med. Inform.*, vol. 2, no. 3, pp. 108–113, 2020, doi: [10.35882/jeeemi.v2i3.4](https://doi.org/10.35882/jeeemi.v2i3.4).
- [15] D. Priyambodo and A. T. Nugraha, “Design and build a photovoltaic and vertical savonius turbine power plant as an alternative power supply to help save energy in skyscrapers,” *J. Electron., Electromed. Eng., Med. Inform.*, vol. 3, no. 1, pp. 57–63, 2021, doi: [10.35882/jeeemi.v3i1.9](https://doi.org/10.35882/jeeemi.v3i1.9).
- [16] S. Qazi, *Standalone Photovoltaic (PV) Systems for Disaster Relief and Remote Areas*. New York, U.S.A.: Elsevier, 2017.
- [17] A. R. Kadafi, “Implementasi sistem temu kembali informasi pada dokumen mutu,” *J. ELTIKOM: J. Tek. Elektr., Teknol. Inf. Komput.*, vol. 2, no. 1, pp. 18–25, 2018, doi: [10.31961/eltikom.v2i1.38](https://doi.org/10.31961/eltikom.v2i1.38).
- [18] A. T. N. Angga, M. J. Shiddiq, and M. F. Ramadhan, “Use ordinary expressions to learn how to extract code feedback from the software program upkeep process,” *Int. J. Adv. Data Inf. Sys.*, vol. 2, no. 2, pp. 105–113, 2021, doi: [10.25008/ijadis.v2i2.1219](https://doi.org/10.25008/ijadis.v2i2.1219).
- [19] V. Reddy, P. S. Varma, and A. Govardhan, “Action model prediction and analysis for CBMR application,” in *2018 Second Int. Conf. Comput. Method. Commun. (ICCMC)*, Erode, India, 15–16 Feb. 2018, pp. 1015–1020, doi: [10.1109/ICCMC.2018.8487504](https://doi.org/10.1109/ICCMC.2018.8487504).
- [20] E. Noei and A. Heydarnoori, “EXAF: A search engine for sample applications of object-oriented framework-provided concepts,” *Inf. Softw. Technol.*, vol. 75, pp. 135–147, 2016, doi: [10.1016/j.infsof.2016.03.007](https://doi.org/10.1016/j.infsof.2016.03.007).
- [21] C. C. Silva, M. Galster, and F. Gilson, “Topic modeling in software engineering research,” *Empir. Softw. Eng.*, vol. 26, no. 6, pp. 1–62, 2021, doi: [10.1007/s10664-021-10026-0](https://doi.org/10.1007/s10664-021-10026-0).
- [22] A. R. Santos, I. C. Machado, E. S. de Almeida, J. Siegmund, and S. Apel, “Comparing the influence of using feature-oriented programming and conditional compilation on comprehending feature-oriented software,” *Empir. Softw. Eng.*, vol. 24, no. 3, pp. 1226–1258, 2019, doi: [10.1007/s10664-018-9658-x](https://doi.org/10.1007/s10664-018-9658-x).
- [23] N. Gupta, V. Yadav, and M. Singh, “Automated regression test case generation for web application: A survey,” *ACM Comput. Surveys (CSUR)*, vol. 51, no. 4, pp. 1–25, 2018, doi: [10.1145/3232520](https://doi.org/10.1145/3232520).
- [24] E. E. Ogheneovo, “On the relationship between software complexity and maintenance costs,” *J. Comput. Commun.*, vol. 2, no. 14, p1, 2014, doi: [10.4236/jcc.2014.214001](https://doi.org/10.4236/jcc.2014.214001).

- [25] O. Browne, P. O'Reilly, M. Hutchinson, and N. B. Krdzavac, "Distributed data and ontologies: An integrated semantic web architecture enabling more efficient data management," *J. Assoc. Inf. Sci. Technol.*, vol. 70, no. 6, pp. 575–586, 2019, doi: [10.1002/asi.24144](https://doi.org/10.1002/asi.24144).
- [26] S. K. Narayanasamy, K. Srinivasan, Y. C. Hu, S. K. Masilamani, and K. Y. Huang, "A contemporary review on utilizing semantic web technologies in healthcare, virtual communities, and ontology-based information processing systems," *Electronics*, vol. 11, no. 3, p. 453, 2022, doi: [10.3390/electronics11030453](https://doi.org/10.3390/electronics11030453).
- [27] X. Sun, X. Liu, Y. Duan, and B. Li, "Using hierarchical latent dirichlet allocation to construct feature tree for program comprehension," *Sci. Program.*, vol. 2017, p. 4382348, 2017, doi: [10.1155/2017/4382348](https://doi.org/10.1155/2017/4382348).
- [28] M. Landhäußer, S. J. Körner, and W. F. Tichy, "From requirements to UML models and back: How automatic processing of text can support requirements engineering," *Softw. Qual. J.*, vol. 22, no. 1, pp. 121–149, 2014, doi: [10.1007/s11219-013-9210-6](https://doi.org/10.1007/s11219-013-9210-6).